

## Double Pancake Bonds: Pushing the Limits of Strong $\pi$ – $\pi$ Stacking Interactions

Zhong-hua Cui,<sup>†</sup> Hans Lischka,<sup>‡,§</sup> Habtamu Z. Beneberu,<sup>†,||</sup> and Miklos Kertesz<sup>\*,†</sup>

<sup>†</sup>Department of Chemistry, Georgetown University, 37th and O Streets, NW, Washington, D.C. 20057-1227, United States

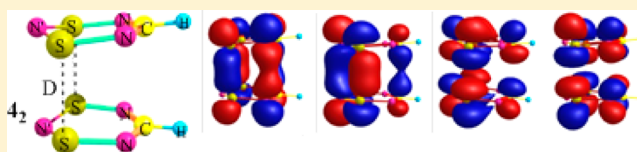
<sup>‡</sup>Department of Chemistry and Biochemistry, Texas Tech University, Lubbock, Texas 79409-1061, United States

<sup>§</sup>Institute for Theoretical Chemistry, University of Vienna, A-1090 Vienna, Austria

<sup>||</sup>Department of Chemistry, University of the District of Columbia, Washington, D.C. 20008, United States

### **S** Supporting Information

**ABSTRACT:** The concept of a double-bonded pancake bonding mechanism is introduced to explain the extremely short  $\pi$ – $\pi$  stacking contacts in dimers of dithiatriazines. While ordinary single pancake bonds occur between radicals and already display significantly shorter interatomic distances in comparison to van der Waals (vdW) contacts, the double-bonded pancake dimer is based on diradicaloid or antiaromatic molecules and exhibits even shorter and stronger intermolecular bonds that breach into the range of extremely stretched single bonds in terms of bond distances and binding energies. These properties give rise to promising possibilities in the design of new materials with high electrical conductivity and for the field of spintronics. The analysis of the double pancake bond is based on cutting edge electron correlation theory combining multireference (nondynamical) effects and dispersion (dynamical) contributions in a balanced way providing accurate interaction energies and distributions of unpaired spins. It is also shown that the present examples do not stand isolated but that similar mechanisms operate in several analogous nonradical molecular systems to form double-bonded  $\pi$ -stacking pancake dimers. We report on the amazing properties of a new type of stacking interaction mechanism between  $\pi$  conjugated molecules in the form of a “double pancake bond” which breaks the record for short intermolecular distances and provides formidable strength for some  $\pi$ – $\pi$  stacking interactions.



These properties give rise to promising possibilities in the design of new materials with high electrical conductivity and for the field of spintronics. The analysis of the double pancake bond is based on cutting edge electron correlation theory combining multireference (nondynamical) effects and dispersion (dynamical) contributions in a balanced way providing accurate interaction energies and distributions of unpaired spins. It is also shown that the present examples do not stand isolated but that similar mechanisms operate in several analogous nonradical molecular systems to form double-bonded  $\pi$ -stacking pancake dimers. We report on the amazing properties of a new type of stacking interaction mechanism between  $\pi$  conjugated molecules in the form of a “double pancake bond” which breaks the record for short intermolecular distances and provides formidable strength for some  $\pi$ – $\pi$  stacking interactions.

### 1. INTRODUCTION

$\pi$ -Stacking in radical dimers, some of which are illustrated in Chart 1 in the form of the constituent monomers, is responsible for the formation of a very interesting class of chemical compounds which display favored packing geometries as described by the maximum multicenter overlap principle between neighboring molecules.<sup>1</sup> This preferred orientation is primarily due to the energy lowering of the singly occupied molecular orbital (SOMO) of the radical as it overlaps with its neighbor. This SOMO–SOMO stabilization can be rationalized by the simple molecular orbital (MO) diagram shown in Chart 2a in which the bonding highest occupied molecular orbital (HOMO) is doubly occupied. For example, for the prototypical phenalenyl (PHY, **1**) dimer **1<sub>2</sub>**, the efficient  $\pi$ – $\pi$  overlap provides the driving force for the stabilization of the dimer<sup>2</sup> which is responsible for contact distances significantly shorter and interaction energies larger than those for typical van der Waals (vdW) interactions.<sup>3–8</sup> The term “pancake bonding” has been suggested for this type of bonding.<sup>9,10</sup> A major motivation in making and understanding these  $\pi$ -stacking pancake interactions originates in the quest to make new molecular materials with high electrical conductivity<sup>2</sup> and for spintronics.<sup>11</sup> A crucial condition for the suitability of  $\pi$ -stacked molecules for such purposes is a strong overlap and thus a strong interaction and a short intermolecular bonding distance

between the stacked subsystems. High electrical conductivities have been achieved for systems with various derivatives of **1**, **2**, and other  $\pi$ -stacking materials.<sup>2,12</sup> However, there is a strong need to push the limits of pancake interactions to even shorter distances and stronger interactions in order to offer new opportunities for materials design.

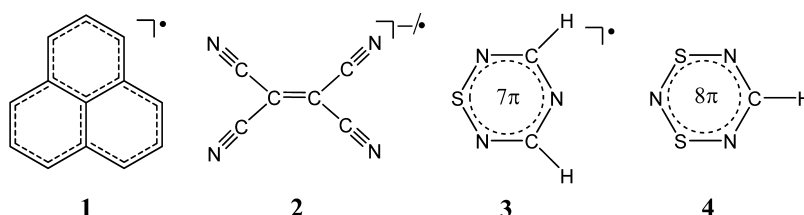
Therefore, is there a possibility to create even stronger pancake bonds and more attractive interactions? In fact, the answer is yes as the dimer orbital diagrams, shown in Chart 2b or 2c, demonstrate. They are based on a monomer with a triplet or a singlet diradicaloid ground state with a low-lying triplet state in the latter case in combination with an antiaromatic electron count ( $8\pi$ ) and antiaromatic character.<sup>13</sup> If such a situation exists, a double pancake bonding could arise as a four electron/multicenter ( $4e/mc$ ) bonding interaction with a formal bond order  $p_{MO}$  of 2 since two bonding orbitals are doubly occupied. In general we compute the bond order  $p_{MO}$  at the MO diagram level as

$$p_{MO} = \frac{1}{2}(N_{\text{bind}} - N_{\text{anti}}) \quad (1)$$

Received: June 4, 2014

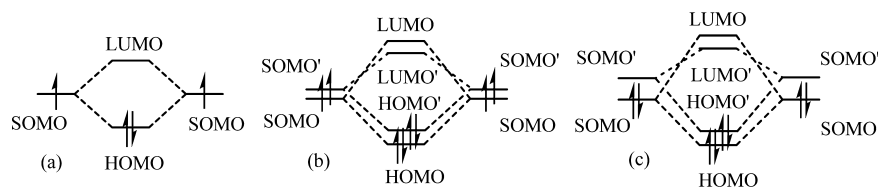
Published: August 24, 2014

Chart 1. Molecules Discussed: Phenalenyl Radical (1), Tetracyanoethylene Radical Anion (2), 1,2,4,6-Thiatriazine Radical (3), and 1,3,2,4,6-Dithiatriazine (4)<sup>a</sup>



<sup>a</sup>1–3 form single-bonded pancake dimers; 4 forms double-bonded pancake dimers.

Chart 2. (a) Molecular Orbital Diagram for Single Pancake-Bonded Dimers; (b) Molecular Orbital Diagram for Double Pancake-Bonded Dimers Based on a Triplet Ground State of the Monomer; (c) Molecular Orbital Diagram for Double Pancake-Bonded Dimer Based on a Singlet Diradicaloid Ground State of the Monomer with a Low HOMO–LUMO Gap<sup>a</sup>



<sup>a</sup>The formal bond order according to eq 1 is 1 for 1<sub>2</sub>, 2<sub>2</sub>, and 3<sub>2</sub> (single-bonded pancake) and 2 for 4<sub>2</sub> (double-bonded pancake).

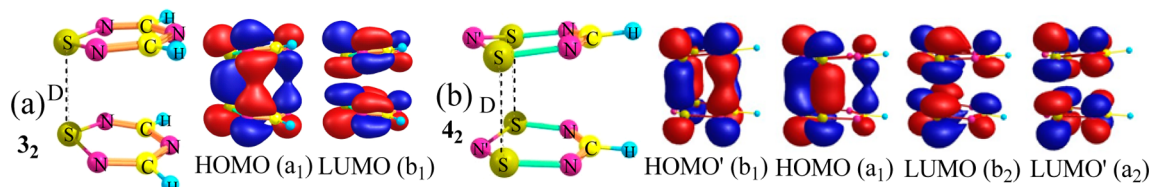


Figure 1. Illustration of the bonding and antibonding combinations of the two and four SOMOs for 3<sub>2</sub> (a) and 4<sub>2</sub> (b), respectively. D is the short intermolecular sulfur–sulfur contact, D<sub>S–S</sub>.

where  $N_{\text{bind}}$  is the number of electrons in the bonding orbitals and  $N_{\text{anti}}$  is the number of electrons in antibonding orbitals.

The (4e/mc) bond would lead to a significant improvement in terms of the interaction strength in contrast to the formal bond order of 1 for 1<sub>2</sub> as indicated by Chart 2. Antiaromatic compounds are usually characterized by low stability which makes the search for appropriate candidates for the double pancake bond difficult. Nevertheless, appropriate compounds should exist. A good example is given in the Cambridge Structural Database, CSD,<sup>14</sup> in the form of the phenyl derivative<sup>15</sup> and the 4-chlorophenyl derivative<sup>16</sup> of 1,3,2,4,6-dithiatriazine, 4, where the phenyl and 4-chlorophenyl have been replaced by H. It will be compared to an analogous stable 7 $\pi$ -electrons radical, 1,2,4,6-thiatriazine,<sup>17</sup> 3, that forms a traditional 2e/mc bonded pancake bond. 1,3,2,4,6-Dithiatriazine (4) is a neutral molecule with 8 $\pi$ -electrons which forms a very short pancake bonded dimer according to its crystal structure.<sup>15</sup>

Can the 1,3,2,4,6-dithiatriazine dimer really be viewed as an example for the double pancake bond, and, if so, what can we learn from it for the construction of other and possibly better examples? To answer these questions from a theoretical point of view in a thorough way one has to go well beyond the simple MO schemes presented so far. It is crucial to understand the subtle interplay of two kinds of electron correlation effects which make these  $\pi$ -stacking interactions so challenging to understand and design. On one side there is the quasi-degeneracy of the HOMO and LUMO calling for multi-

reference methods for an adequate description whereas on the other side dynamical correlation effects are essential for the description of vdW interactions.

It is the purpose of this contribution to resolve the question of the energetic feasibility of a double pancake bond using the high-level multireference average quadratic coupled cluster, MR-AQCC, theory.<sup>18</sup> This level of theory provides an excellent approach to the simultaneous treatment of static and dynamic electron correlation. It has been successfully used previously in interpreting the bonding characteristics of the phenalenyl dimer<sup>19</sup> and the TCNE<sup>−</sup> anion dimer,<sup>3</sup> two prototypical examples of pancake bonding. The multireference starting point assures that the multiradical character is included in the theory from the outset, and the approximate coupled cluster level assures that the millions of configurations necessary for the dispersion interaction are well accounted for.<sup>20–22</sup>

## 2. METHODS AND MODELS

**2.1. Computational Details.** Complete active space self-consistent field (CASSCF)<sup>23</sup> and multireference averaged coupled cluster MR-AQCC<sup>18/6-311++G(2d,2p)</sup><sup>24</sup> calculations including full geometry optimizations were carried out on the  $\pi$  dimers 3<sub>2</sub> and 4<sub>2</sub>. The electronic state configurations of these two  $\pi$  dimers with  $C_{2v}$  symmetry are illustrated in Figure 1. The CASSCF(2,2) (3<sub>2</sub>) and CASSCF(4,4) (4<sub>2</sub>) calculations have been performed using the bonding and antibonding orbitals of the SOMOs in 3 and 4 as the active orbital space for 3<sub>2</sub> and 4<sub>2</sub>  $\pi$  dimers, respectively. Molecular orbitals (MOs) created by the CASSCF method were used in the MR-AQCC calculations including gradients with the same active orbital

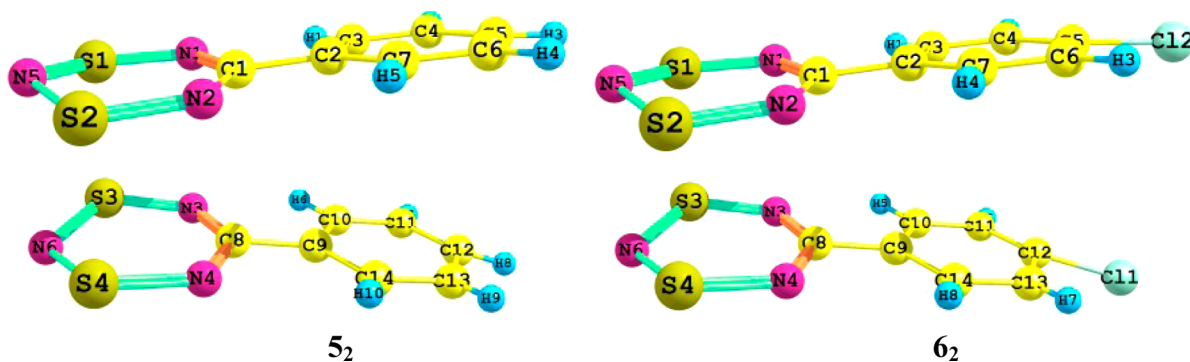
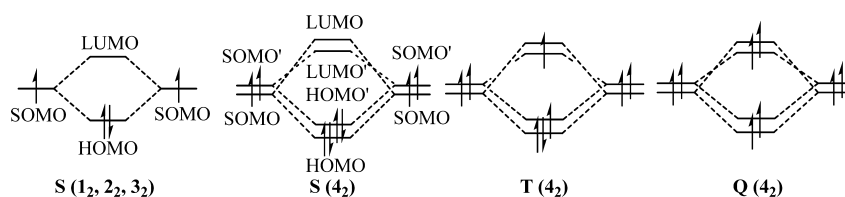


**Figure 2.** Structures of two substituted dithiatiazine ( $\text{HCN}_3\text{S}_2$ )  $\pi$  dimers indicate close similarity in their structures. These dimers were excised from their respective crystal structures: the phenyl derivative<sup>15</sup> ( $5_2$ ) and the 4-chlorophenyl derivative<sup>16</sup> ( $6_2$ ) are derivatives of 1,3,2,4,6-dithiatiazine, 4.

**Chart 3.** MO Diagrams for the Dimers of Various States of  $1_2$ ,  $2_2$ ,  $3_2$ , and  $4_2^a$



<sup>a</sup>States are designated as S for singlet, T for triplet, and Q for quintet.

spaces as used in the CASSCF calculations. The total space of configuration state functions (CSFs) was constructed by applying single and double excitations from valence orbitals to all virtual orbitals for all reference CSFs and imposing generalized interacting space restrictions.<sup>25</sup> The 1s core orbitals of the C, N, and S atoms and 2s and 2p orbitals of the S atoms were frozen throughout all MR-AQCC calculations (additionally, eight low-lying occupied orbitals were frozen in  $4_2$ ). The analysis of the radical character of the complexes was performed by analyzing (i) the natural orbitals (NOs) of the one-particle MR-AQCC density matrix and (ii) the effectively unpaired density using the nonlinear formula of Head-Gordon.<sup>32</sup> Atomic values are based on a Mulliken analysis for the unpaired density. The COLUMBUS suite of programs was used for the MR-AQCC and CASSCF computations.<sup>26</sup> In addition to the single state CASSCF(4,4) approach for the singlet and quintet states, state averaged CASSCF calculations have been performed on the triplet state dominated by two main configurations:  $\Phi_1 = | \dots a_1^2 b_1^1 a_2^1 b_2^0 |$  and  $\Phi_2 = | \dots b_1^2 a_1^1 b_2^1 a_2^0 |$ . Density functional theory (DFT) was used to supplement the MR-AQCC calculations for three candidate molecules that are promising for double pancake bonding. Substitution effects were assessed by DFT calculations.

Figures 2 and S1 compare the crystallographic data for the two experimentally observed derivatives of the double bonded pancake dimer  $4_2$ . The phenyl and chlorophenyl substitution has little effect on the geometry of the dithiatiazine core validating the use of  $4_2$  as a good model for these experimentally observed systems.

For the cationic dimers the Coulomb energy was estimated by using the following formula based on the approximate  $Q_i$  atomic charges. We use  $Q_i$  values based on electrostatic potentials (ESP) following the Hu–Lu–Yang charge fitting method (HLY scheme)<sup>27</sup> in eq 2<sup>28</sup>

$$E_{\text{Coul}} = \sum_{i < j} Q_i Q_j / R_{i,j} - C \quad (2)$$

in which  $C$  is taken as the reference Coulomb energy at  $D = 10.0 \text{ \AA}$ .

The interaction energy  $E_{\text{int}}(D)$  of the dimer with intermolecular separation  $D$  between the monomers is computed at the MR-AQCC level, as the energy of the complex with reference to the energy at a separation of  $D = 10.0 \text{ \AA}$  where the overlap is sufficiently close to zero:

$$E_{\text{int}}(D) = E_{\text{Total}}(D) - E_{\text{Total}}(10.0 \text{ \AA}) \quad (3)$$

Further computational details are given in the Supporting Information section.

**2.2. Approximate Separation of the Interaction Energy: vdW and Pancake Bonding Components.** The separation of the vdW and the attractive SOMO–SOMO interaction is essential for the analysis of the interaction energy,  $E_{\text{int}}(D)$ . It is written as the sum of the specific pancake  $\pi$ – $\pi$  bonding SOMO–SOMO interaction ( $E_{\text{SOMO–SOMO}}$ ) and the van der Waals ( $E_{\text{vdW}}$ ) term<sup>3,6,7</sup>

$$E_{\text{int}}(D) = E_{\text{SOMO–SOMO}}(D) + E_{\text{vdW}}(D) \quad (4)$$

The vdW term includes dispersion, Pauli repulsion, and electrostatic interactions.  $E_{\text{vdW}}$  is approximated by the interaction energy  $E_{\text{int}}^{\text{HS}}$ .

$$E_{\text{vdW}}(D) \approx E_{\text{int}}^{\text{HS}}(D) \quad (5)$$

computed for the high-spin (HS) state taken at the same distance  $D$  since in this case bonding and antibonding interactions derived from the SOMO orbitals approximately cancel and  $p_{\text{MO}} = 0$  (eq 1).<sup>3,7,19</sup>

According to Chart 3, for  $4_2$  the singlet (S), triplet (T), and quintet (Q) states contain double, single, and no pancake bond character with formal bonders  $p_{\text{MO}}$  equal to 2, 1, and 0, respectively (eq 1). The singlet states of  $1_2$ ,  $2_2$ , and  $3_2$  all possess a bond order  $p$  of 1. The SOMO–SOMO interaction term for both the single and double pancake bond, respectively, is then approximated as follows:

$$E_{\text{SOMO–SOMO}}(D) = E_{\text{int}}^{\text{LS}}(D) - E_{\text{int}}^{\text{HS}}(D) \quad (6)$$

LS labels the respective low spin state which is only singlet for  $1_2$ ,  $2_2$ , and  $3_2$  but can be singlet or triplet for  $4_2$ . The high-spin state is triplet in the former case and quintet in the latter. A version of this approximation restricted to LS = singlet and HS = triplet has been used by Mota et al.<sup>7</sup> for the analysis of the interaction energy of pancake bonded dimers of **1** and **2** and has been recently validated for both of these systems within the context of the MR-AQCC level of theory.<sup>3,19</sup> One result, relevant for this study, was that the vdW term becomes repulsive at the short contacts typical for pancake bonds. According to this analysis, the pancake contacts shorter than the typical vdW distance result from the large negative (bonding)  $E_{\text{SOMO–SOMO}}$  pancake interaction.

## 3. RESULTS AND DISCUSSION

**3.1. Computed Interaction Energies and Its Components of  $3_2$  and  $4_2$ .** Total energy minimization of the dimer structures at the MR-AQCC level followed by rigid scans as a function of the shortest sulfur...sulfur distance ( $D_{S-S}$ ) were performed for the  $\pi$ -stacking pancake dimers  $3_2$  and  $4_2$ . The resulting interaction energies are presented in Figure 3a and 3b, while the derived  $E_{\text{SOMO-SOMO}}$  pancake bonding energy terms based on eq 6 are shown Figure 3c.

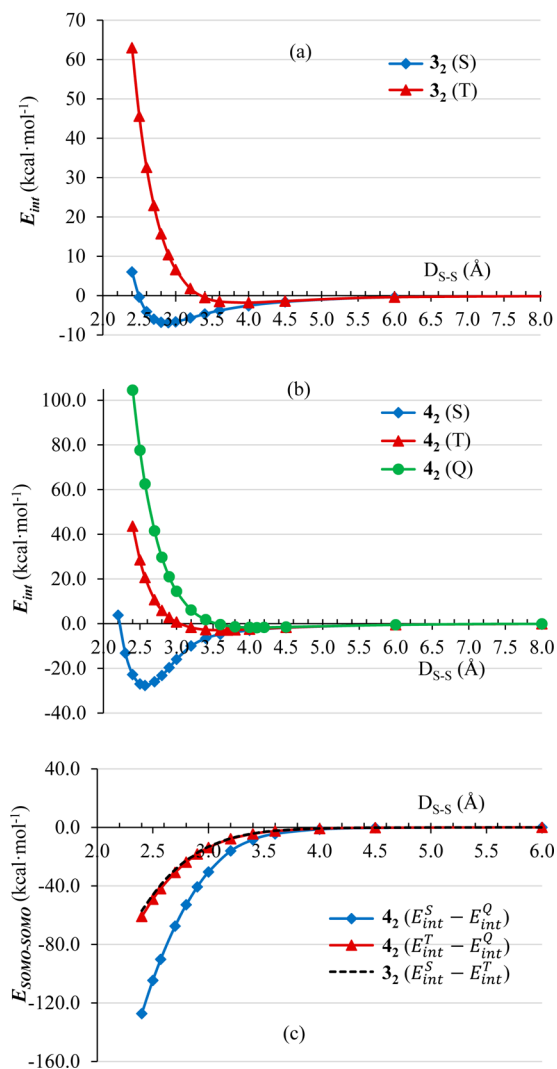


**Figure 3.** Potential energy scans for (a) the singlet and triplet states of  $3_2$  and (b) the singlet, triplet, and quintet states of  $4_2$ . The SOMO-SOMO interaction energies are represented in (c) and are defined in the inset according to eq 6. Computations refer to  $C_{2v}$  symmetry using an MR-AQCC/6-311++G(2d,2p) level of theory.

The fully optimized geometries and the respective interaction energies are discussed first; key data are collected in Table 1. The singlet minimum of the single pancake bonded  $3_2$  shows an interaction energy of  $-7.0$  kcal/mol at  $D_{S-S} = 2.870$  Å. This distance is much shorter than the vdW distance of  $3.60$  Å<sup>29</sup> and is clearly indicative of pancake bonding. The experimentally observed contact for the dimers of the diphenyl substituted **3** in the crystal is  $2.677$  Å (CSD refcode CUVTAO).<sup>17</sup> The agreement between computation and experiment is good, given the missing steric repulsions due to the phenyls in the model

**Table 1.** Computed<sup>a</sup> Interaction Energies,  $E_{\text{int}}$ , and Its Components,  $E_{\text{vdW}}$  and  $E_{\text{SOMO-SOMO}}$

species <sup>b</sup>	$D^c$ (Å)	$E_{\text{int}}$ (kcal/mol)	$E_{\text{vdW}}$ (kcal/mol)	$E_{\text{SOMO-SOMO}}$ (kcal/mol)
$1_2$ (S)	3.104 <sup>d</sup>	-11.5	5.7	-17.2
$1_2$ (T)	3.676 <sup>e</sup>	-3.3	-3.3	0.0
$1_2$ (T)	3.104 <sup>f</sup>	5.7	5.7	0.0
$2_2$ (S)	2.735 <sup>d</sup>	-10.1	13.0	-23.1
$2_2$ (T)	3.820 <sup>e</sup>	-2.7	-2.7	0.0
$2_2$ (T)	2.735 <sup>f</sup>	13.0	13.0	0.0
$3_2$ (S)	2.870 <sup>d</sup>	-7.0	11.8	-18.8
$3_2$ (T)	4.0 <sup>g</sup>	-1.8	-1.8	0.0
$3_2$ (T)	2.870 <sup>f</sup>	11.8	11.8	0.0
$4_2$ (S)	2.571 <sup>d</sup>	-27.7	62.5	-90.2
$4_2$ (T)	3.6 <sup>g</sup>	-2.9	-0.4	-2.5
$4_2$ (Q)	2.571 <sup>f</sup>	62.5	62.5	0.0
$4_2$ (Q)	3.6 <sup>g</sup>	-0.4	-0.4	0.0
$4_2$ (Q)	4.1 <sup>h</sup>	-1.8	-1.8	0.0

<sup>a</sup>MR-AQCC/6-311++G(2d,2p) level of theory. Data for  $1_2$  are from ref 19 and for  $2_2$  from ref 3. <sup>b</sup>S, T, and Q stand for singlet, triplet, and quintet states, respectively. <sup>c</sup> $D$  represents C-C contacts for  $1_2$  and  $2_2$  and S-S contacts for the rest of the dimers. <sup>d</sup>Optimized geometry of the singlet (S) dimer. <sup>e</sup>Optimized geometry of the triplet (T) dimer. <sup>f</sup>Computed high-spin state using the singlet ground state geometry of the dimer. <sup>g</sup>Minimum on the rigid D scan for the triplet (T) dimer. <sup>h</sup>Minimum on the rigid D scan for the quintet (Q) dimer.

compound used and due to intermolecular interactions in the crystal also not included in the calculations. The interaction energy for the triplet state of  $3_2$  at the equilibrium geometry of the singlet ( $D_{S-S} = 2.870$  Å) is repulsive with  $+11.8$  kcal/mol, a value which is used to approximate  $E_{\text{vdW}}$  at this distance according to eq 5. The SOMO-SOMO binding energy of  $3_2$  is  $-18.8$  kcal/mol at the equilibrium geometry computed from eq 6 and represents a significant attraction. On the other hand, the modest attraction of  $-1.8$  kcal/mol at the minimum distance  $D_{S-S}$  of  $4.0$  Å for the triplet state of  $3_2$  corresponds well to what is expected of pure vdW interactions in terms of both the location and depth of the minimum.

Turning to the double pancake case of  $4_2$ , the singlet minimum shows a much larger interaction energy of  $-27.7$  kcal/mol at a remarkably short contact distance of  $D_{S-S} = 2.571$  Å (Table 1). This distance is considerably shorter (by  $0.3$  Å) than in the radical dimer  $3_2$  discussed above and by more than  $1$  Å shorter than the vdW distance of  $3.60$  Å.<sup>29</sup> The experimentally observed  $D_{S-S}$  distance for the dimers of the phenyl substituted **4** in the crystal is  $2.529$  Å (average of two values from CSD, refcode DESSID).<sup>15</sup> The value in the isostructural 4-chlorophenyl derivative dimer is  $2.522$  Å (average of two values from CSD, refcode PAFLAJ)<sup>16</sup> which is still much longer than the typical single S-S bond of about  $2.04$  Å.<sup>16</sup> The agreement between computation and experiment is very good, and again the differences are largely attributable to steric repulsions due to the two phenyls (not present in the computations) and to intermolecular interactions in the crystal. The vdW interaction energy computed from eq 5 using the quintet at the equilibrium geometry of the singlet is repulsive with  $+62.5$  kcal/mol. This very large positive value indicates that the SOMO-SOMO interaction for the singlet with such a short distance must more than overcome this repulsive term. The development of the SOMO-SOMO pancake bonding energy according to eq 6 with the intermolecular distance  $D_{S-S}$  is shown in Figure 3c. At the equilibrium geometry of the

singlet of  $4_2$  it reaches the amazingly large attractive value of  $-90.2$  kcal/mol. For comparison, according to Figure 3b and Table 1 the modest attraction of  $-1.8$  kcal/mol at the minimum  $D = 4.1$  Å of the quintet corresponds well to what is expected of purely vdW interactions.

The triplet interaction energy curve for  $4_2$  in Figure 3b shows an intermediate behavior between that of the singlet and quintet with a minimum at  $3.6$  Å and an interaction energy of  $-2.9$  kcal/mol. The triplet state is used as a tool to connect the single- and double-bonded pancake interactions in  $4_2$ . The bare SOMO–SOMO pancake bonding energy term for the triplet of  $4_2$  (Figure 3c) coincides remarkably well with that of the typical pancake bonded dimer of  $3_2$ . As has been discussed in connection with Chart 3, in the triplet state of  $4_2$  only one pancake bond is left over as compared to the singlet, and therefore it agrees well with the singlet of  $3_2$ , which also represents one pancake bond.

The dissociation limit of the  $4_2$  dimer yields three degenerate states (S, T, and Q). They arise from the coupling of the two triplet monomers as discussed in the Supporting Information section S.IV. There is also a lower energy singlet of the monomer that shows signs of a second order Jahn–Teller symmetry breaking.<sup>13</sup>

**3.2. Diradical Characters and Unpaired Density Analysis.** The extent and character of unpaired density of the complexes were analyzed by the natural orbitals (NOs) of the one-particle MR-AQCC density matrix and the effectively unpaired electron density,<sup>30–32</sup> which provides a measure for the separation of an electron pair into different spatial regions. The total number of effectively unpaired electrons ( $N_U$ ) is computed with the following formula:<sup>32</sup>

$$N_U = \sum_{i=1}^N n_i^2 (2 - n_i)^2 \quad (7)$$

where  $n_i$  refers to the  $i$ -th natural orbital occupancy and  $N$  to the number of natural orbitals. We have selected the nonlinear formula given in ref 32 since it reduces the relative contributions of the  $n_i$  values that are close to 0 or 2 diminishing the contributions from dynamical correlation and thus highlighting only the truly open-shell contributions of the radical centers.

The total number of effectively unpaired electrons,  $N_U$ , is displayed in Figure 4a as a function of the S··S contact distance ( $D_{S-S}$ ) for the different multiplicities of  $4_2$  and the singlet state of  $3_2$ . At large separations  $N_U$  values around  $4.28 e$  are obtained for  $4_2$  exceeding the expected  $4.0 e$  because at the MR-AQCC level, in addition to the two unpaired electrons on each of the two monomers, dynamical correlations provide a slight excess over  $4.0 e$ . As the contact distance is reduced, the singlet  $N_U$  is dramatically reduced as the electrons start to pair. At the equilibrium  $D = 2.571$  Å the pairing is still incomplete where  $N_U = 0.57 e$  indicates a remaining limited polyradical<sup>33</sup> character. The triplet  $N_U$  values of  $3_2$  are not shown; they are essentially constant at  $\sim 2.4 e$ , representing the two unpaired electrons plus some contributions from dynamical correlation. At large separations the singlet state of  $3_2$  has the same number of unpaired electrons as the triplet, which, however, in the former case is substantially reduced as the two-electron pancake bond is being formed. At the equilibrium geometry ( $D = 2.870$  Å) the  $N_U = 0.93 e$  value indicates a still existent significant diradicaloid character, typical for such single pancake bonds.<sup>3,34</sup> The qualitative difference compared to the single-bonded

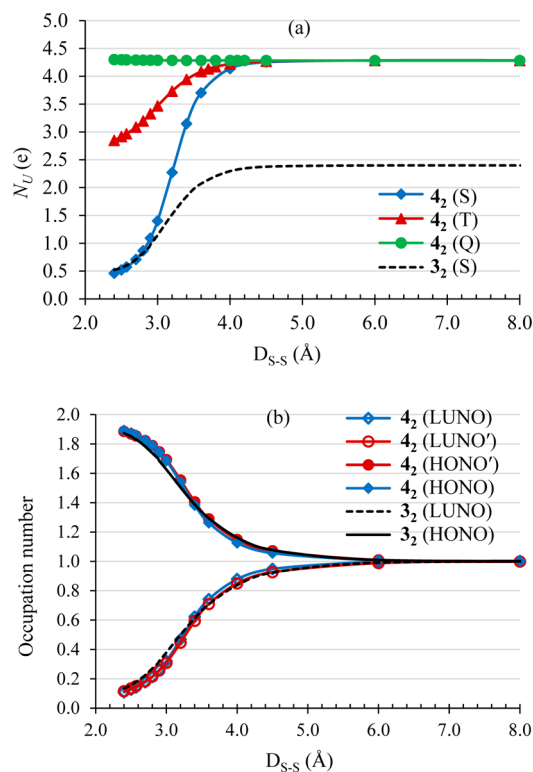


**Figure 4.** (a) Total number of effectively unpaired electrons ( $N_U$ ) of  $3_2$  and  $4_2$  and (b) occupation numbers of the frontier NOs of the singlet states of  $3_2$  and  $4_2$  as a function of the separation distance ( $D_{S-S}$ ).

pancake is that the double-bonded pancake bond is substantially shorter, and the multiradical character is reduced. The triplet state of  $4_2$  retains a high value of multiradical character of  $N_U$  near  $3.5 e$  at its minimum of  $D = 3.6$  Å indicating that it is located intermediate between the quintet and singlet in terms of electron pairing.

Figure 4b displays the natural orbital occupation numbers (NOONs) for the relevant frontier orbitals of the dimers  $3_2$  and  $4_2$  shown in Figure 1. The values are nearly equal to 1.0 at large separations as expected. All NOON values are evolving toward 2.0 and 0.0 at a similar pace as  $D$  is reduced. However, at the respective equilibrium distance of each molecule these values differ significantly since the  $D_{S-S}$  distance is considerably smaller for the double-bonded  $4_2$  pancake as compared to the single-bonded  $3_2$  pancake.

The unpaired electron densities, shown in Figure 5, indicate this difference also: the radical character of the double-bonded  $4_2$  pancake is much smaller as compared to the single-bonded  $3_2$  case.

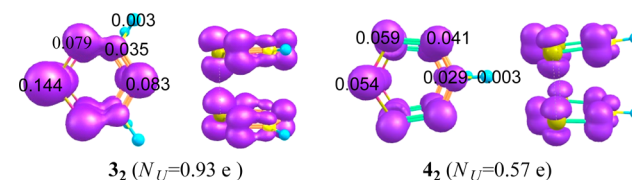


**Figure 5.** Effectively unpaired electron density (isovalue 0.002 au) and atomic contributions for the singlets of  $3_2$  and  $4_2$ .  $N_U$  is the number of effectively unpaired electrons given in parentheses indicating stronger electron pairing in  $4_2$  compared to  $3_2$ .

Extending the simple integer bond order  $p_{MO}$  defined in eq 1, we computed a more detailed bond order  $p_{NO}$  based on the two and four frontier orbital NOONs for  $3_2$  and  $4_2$ , respectively,

$$p_{NO} = (\text{NEBO} - \text{NEABO})/2 \quad (8)$$

where NEBO is the number of electrons in bonding orbitals, NEABO is the number of electrons in the antibonding orbitals based on the natural orbital occupancies for the two frontier orbitals for  $3_2$  and four frontier orbitals for  $4_2$ , respectively. The  $p_{NO}$  values obtained are 0.695 for  $3_2$  and 1.715 for  $4_2$ . This reflects a major difference in the occupancies, which mirror the much stronger and shorter pancake bonds in the  $\pi$ -stacking dimer  $4_2$  compared to those in the radical dimer  $3_2$ .

**3.3. Further Examples of Double Pancake Bonded Dimers.** Based on these insights we have designed three new double pancake bonded dimers each with an even number of  $\pi$ -electrons. These systems that might exhibit double pancake bonding were obtained by substituting Se for S in 4 and substituting  $S^+$  for CH in 4, respectively, arriving in both cases at isoelectronic  $8\pi$ -electron rings. A further example is based on the  $C_5H_5^+$  ring that has a triplet ground state with  $D_{3h}$  symmetry and exhibits an antiaromatic electron count. Computational results at the MR-AQCC and UB3LYP levels indicate that these systems exhibit very short intermolecular  $\pi$ -stacking contacts as expected from double pancake bonding.

**3.3.1. Substitution of Se for S in Dithiatriazine:  $Se_2N_3CH$  with 8  $\pi$ -Electrons.** The optimized geometry of a hypothetical double pancake bonded dimer using UB3LYP/6-311++G(2d,2p) is shown in Figure 6. The UDFT geometry

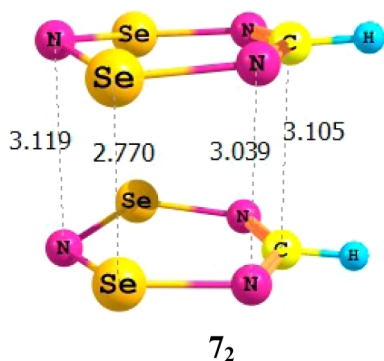


**Figure 6.** Optimized geometry of the Se analogue of  $4_2$  with UB3LYP/6-311++G(2d,2p).

optimization (including UB3LYP and UM06-2X) on the  $(Se_2N_3CH)_2$   $\pi$  dimer ( $7_2$ ) using the 6-311++G(2d,2p) basis set provided strong evidence for double pancake bonding in this dimer. The UDFT methods produced a  $C_{2v}$  symmetry optimized geometry for the  $(Se_2N_3CH)_2$  dimer with intermolecular Se–Se distances of 2.770 Å (UB3LYP) and 2.685 Å (UM06-2X). These contact values are strikingly shorter by 1.030 Å than the vdW distance for Se...Se (3.800 Å).<sup>36</sup> The rest of the intermolecular distances in the  $(Se_2N_3CH)_2$   $\pi$  dimer are similar to those of the  $(S_2N_3CH)_2$   $\pi$  dimer,  $4_2$ . The  $(Se_2N_3CH)_2$   $\pi$  dimer also has a large interaction energy of  $-27.0$  kcal/mol (UB3LYP/6-311++G(2d,2p)) resulting from the perfect SOMO–SOMO overlap, indicating that this unique Se-bearing dimer displays strong double pancake bonding and therefore would be a good candidate for further analysis and perhaps synthesis. The total interaction energy is comparable to that in  $4_2$ :  $-27.0$  indicating the overall strength of the double

pancake bonding and its ability to more than overcome vdW (Pauli) repulsion at these extremely short contact  $\pi$ -stacking distances.

**3.3.2. Substitution of  $S^+$  for CH in Dithiatriazine:  $S_3N_3^+$  with 8  $\pi$ -Electrons.** Two low-lying local minima of the hypothetical double pancake bonded dimer,  $(S_3N_3^+)_2$  ( $8_2$  and  $9_2$ ), were obtained by UB3LYP/6-311++G(2d,2p) and are shown in Figure 7.

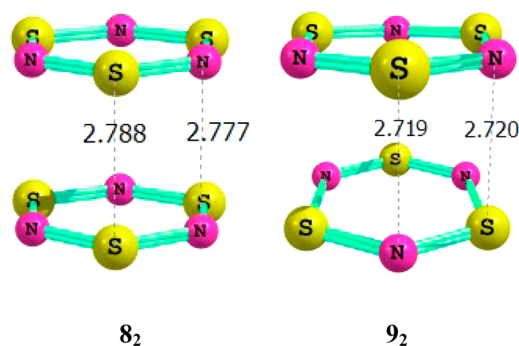


**Figure 7.** Optimized geometry of the  $S^+$  substituted analogue of  $4_2$ ,  $(S_3N_3^+)_2$ . Two configurations are shown with UB3LYP/6-311++G(2d,2p).

The  $8_2$  configuration with perfect overlap was further considered by rigid scan calculations at the MR-AQCC(4,4)/6-311++G(2d,2p) level starting with the UB3LYP/6-311++G(2d,2p) dimer optimized geometry. As shown in Figure 8, the total energy curve ( $E_{int}$ ) indicated that there is a metastable minimum with a significant barrier to dissociation into two  $S_3N_3^+$  fragments, which arises from strong cation–cation Coulomb repulsion. We approximated the corrected (bare)

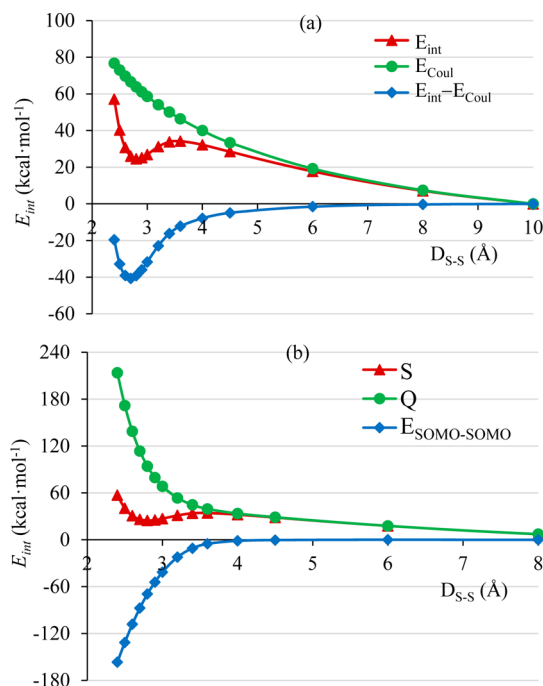
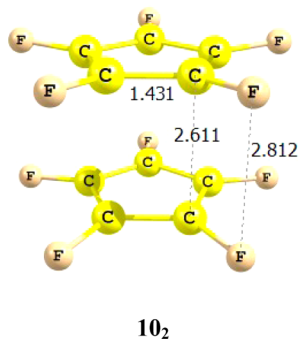


**Figure 8.** Potential energy scans of the singlet and quintet of the  $(S_3N_3^+)_2$   $\pi$  dimer with  $D_{3h}$  symmetry ( $8_2$ ) as a function of the S...S distance ( $D_{S-S}$ ) computed at the MR-AQCC(4,4)/6-311++G(2d,2p) level.

interaction energy as the  $E_{\text{int}} - E_{\text{Coul}}$ . The minimum of this corrected interaction energy of the  $\pi$  dimer is  $-40.7$  kcal/mol at about  $D = 2.7$  Å. Furthermore, the SOMO–SOMO interaction of  $8_2$  has been investigated by subtracting the interaction of the highest spin state (quintet) from the interaction of the singlet state as shown in Figure 8b. It turns out that the  $8_2$  possesses a very significant SOMO–SOMO component in the intermolecular interactions, which is very similar to the behavior of  $4_2$  providing a tremendous driving force toward establishing a double bonded  $\pi$ – $\pi$  stacking pancake.

In the  $8_2$  case the S...S contact was computed to be  $0.812$  Å shorter than the vdW distance after subtracting a large Coulomb repulsion term that was approximated using ESP based approximate point charges. The total interaction energy after subtraction of the Coulomb repulsion is even larger than that for  $4_2$ :  $-27.7$  kcal/mol. The respective  $E_{\text{SOMO-SOMO}}$  value ( $-87.5$  kcal/mol) and the short contacts indicate that the SOMO–SOMO bonding interaction is very strong, and thus further examples of double pancake bonding should be forthcoming.

**3.3.3. Perfluoro-cyclopentadiene Cation:  $C_5F_5^+$  with  $4\pi$ -Electrons.**  $C_5H_5^+$  has the right electron count to be a candidate for double pancake bonding. It has been investigated for its triplet ground state.<sup>35</sup> We turned to the perfluoro derivative of  $C_5H_5^+$ , because we anticipated that the use of  $\sigma$ -electron withdrawing groups will facilitate pancake bond formation.<sup>28</sup> The optimized geometry of the hypothetical double pancake bonded  $\pi$ -dimer,  $(C_5F_5^+)_2$  ( $10_2$ ), using UB3LYP/6-311+G(d) is shown in Figure 9.



$10_2$

**Figure 9.** Optimized geometry of the hypothetical double pancake bonded dimer,  $(C_5F_5^+)_2$ .

$10_2$  exhibits a real local minimum with extremely short  $\pi$ – $\pi$  stacking C–C distances of  $2.611$  Å. The dimer of  $10_2$  represents the first five-member ring forming a double pancake bonded system with two perfectly degenerate SOMO–SOMO interaction terms. Thermodynamically,  $10_2$  is unfavorable because of (i) the strong Coulomb repulsion and (ii) the  $\sigma$  dimer is much more favorable by means of cycloaddition. We suspect that the latter mechanism is a main reason why pancake bonded systems with rings consisting of mostly  $C(sp^2)$  have not yet been characterized. Energy minimization of the singlet ground state of the dimer of the perfluoro derivative of  $C_5H_5^+$  ( $10$ ,  $C_5F_5^+$ ) showed a well-defined local minimum with overall positive interaction energy due to the large Coulomb repulsion. These three examples indicate that it should be possible to find further systems that exhibit double pancake bonding.

## 4. CONCLUSIONS

It has been established for the first time through high-accuracy quantum mechanical modeling that the  $\pi$ -stacking dimer of  $4_2$  can be understood as a double pancake bonded molecular aggregate. This finding enriches the toolkit of chemical interactions in a sensitive area connecting the weak vdW interactions to electron pair chemical bonds. The search for shorter and stronger pancake bonding may lead to intermolecular contacts that might breach into the range of extremely stretched single bonds<sup>37–39</sup> in terms of bond distance and binding energy. The best candidates for utilizing this new double pancake bonding mechanism will be likely found among  $\pi$ -electron rich molecules with their highest two occupied orbitals being of  $\pi$ -type concomitant with either a singlet ground state with a low-lying triplet state and diradicaloid character or  $\pi$ -electron rich molecules with a triplet ground state.

## ■ ASSOCIATED CONTENT

### 📄 Supporting Information

Computational details, validation and convergence of computational modeling, properties of the monomer of 1,3,2,4,6-dithiatiazine ( $4$ ), and absolute energies and the Cartesian coordinates for all the optimized structures concerned. This material is available free of charge via the Internet at <http://pubs.acs.org>.

## ■ AUTHOR INFORMATION

### ✉ Corresponding Author

Kertesz@georgetown.edu

### Notes

The authors declare no competing financial interest.

## ■ ACKNOWLEDGMENTS

We thank the U.S. National Science Foundation for its support of this research at Georgetown University (Grant Number CHE-1006702) and at Texas Tech University (Grant Number CHE-1213263). M.K. is a member of the Georgetown Institute of Soft Matter. Support was also provided by the Robert A. Welch Foundation under Grant No. D-0005 and by the Austrian Science Fund (SFB F41, ViCoM).

## ■ REFERENCES

- (1) Devic, T.; Yuan, M.; Adams, J.; Fredrickson, D. C.; Lee, S.; Venkataraman, D. *J. Am. Chem. Soc.* **2005**, *127*, 14616.
- (2) Haddon, R. C. *ChemPhysChem* **2012**, *13*, 3581.
- (3) Cui, Z.-h.; Lischka, H.; Mueller, T.; Plasser, F.; Kertesz, M. *ChemPhysChem* **2014**, *15*, 165.
- (4) Novoa, J. J.; Miller, J. S. *Acc. Chem. Res.* **2007**, *40*, 189.
- (5) Casado, J.; Burrezo, P. M.; Ramirez, F. J.; López Navarrete, J. T.; Lapidus, S. H.; Stephens, P. W.; Vo, H.-L.; Miller, J. S.; Mota, F.; Novoa, J. J. *Angew. Chem., Int. Ed.* **2013**, *52*, 6421.
- (6) Jung, Y.; Head-Gordon, M. *Phys. Chem. Chem. Phys.* **2004**, *6*, 2008.
- (7) Mota, F.; Miller, J. S.; Novoa, J. J. *J. Am. Chem. Soc.* **2009**, *131*, 7699.
- (8) Tian, Y.-H.; Kertesz, M. *J. Am. Chem. Soc.* **2010**, *132*, 10648.
- (9) Mulliken, R. S.; Person, W. B. *Molecular Complexes*; Wiley & Sons: 1969; Chapter 16.
- (10) Suzuki, S.; Morita, Y.; Fukui, K.; Sato, K.; Shiomi, D.; Takui, T.; Nakasuji, K. *J. Am. Chem. Soc.* **2006**, *128*, 2530.
- (11) Raman, K. V.; Kamerbeek, A. M.; Mukherjee, A.; Atodiresei, N.; Sen, T. K.; Lazić, P.; Caciuc, V.; Michel, R.; Stalke, D.; Mandal, S. K.; Blügel, S.; Müntenberg, M.; Moodera, J. S. *Nature* **2013**, *493*, 509.

- (12) Curtis, M. D.; Cao, J.; Kampf, J. W. *J. Am. Chem. Soc.* **2004**, *126*, 4318.
- (13) Hoffmeyer, R. E.; Chan, W.-T.; Goddard, J. D.; Oakley, R. T. *Can. J. Chem.* **1988**, *66*, 2279.
- (14) Cambridge Structural Database, by Cambridge Crystallographic Data Center, www.ccdc.cam.ac.uk, 2013 (CSD version 5.35, ConQuest version 1.16).
- (15) Boeré, R. T.; French, C. L.; Oakley, R. T.; Cordes, A. W.; Privett, J. A. J.; Craig, S. L.; Graham, J. B. *J. Am. Chem. Soc.* **1985**, *107*, 7710.
- (16) Boeré, R. T.; Fait, J.; Larsen, K.; Yip, J. *Inorg. Chem.* **1992**, *31*, 1417.
- (17) Hayes, P. J.; Oakley, R. T.; Cordes, A. W.; Pennington, W. T. *J. Am. Chem. Soc.* **1985**, *107*, 1346.
- (18) Szalay, P. G.; Bartlett, R. J. *Chem. Phys. Lett.* **1993**, *214*, 481.
- (19) Cui, Z.-h.; Lischka, H.; Beneberu, H. Z.; Kertesz, M. *J. Am. Chem. Soc.* **2014**, *136*, 5539.
- (20) Shepard, R. In *Modern Electronic Structure Theory*; Yarkony, D. R., Ed.; World Scientific: Singapore, 1995; Vol. 1, p 345.
- (21) Shepard, R.; Lischka, H.; Szalay, P. G.; Kovar, T.; Ernzerhof, M. *A. J. Chem. Phys.* **1992**, *96*, 2085.
- (22) Lischka, H.; Dallos, M.; Shepard, R. *Mol. Phys.* **2002**, *100*, 1647.
- (23) (a) Ruedenberg, K.; Cheung, L. M.; Elbert, S. T. *Int. J. Quantum Chem.* **1979**, *16*, 1069. (b) Roos, B. O. *Adv. Chem. Phys.* **1987**, *69*, 399.
- (24) (a) McLean, A. D. *J. Chem. Phys.* **1980**, *72*, 5639. (b) Krishnan, R.; Binkley, J. S.; Seeger, R.; Pople, J. A. *J. Chem. Phys.* **1980**, *72*, 650.
- (25) Bunge, A. *J. Chem. Phys.* **1970**, *53*, 20.
- (26) Lischka, H.; Müller, T.; Szalay, P. G.; Shavitt, I.; Pitzer, R. M.; Shepard, R. *COLUMBUS – A Program System for Advanced Multireference Theory Calculations*; Allen, W., Ed.; Wiley Interdisciplinary Reviews: Computational Molecular Science (WIREs:CMS); Wiley & Sons: 2011; Vol. 1, pp 191–199. Lischka, H.; et al. COLUMBUS, an ab initio electronic structure program. Release 7.0, 2013, www.univie.ac.at/columbus.
- (27) Hu, H.; Lu, Z.; Yang, W. *J. Chem. Theory Comput.* **2007**, *3*, 1004.
- (28) Tian, Y. H.; Kertesz, M. *J. Phys. Chem. A* **2011**, *115*, 13942.
- (29) Bondi, A. *J. Phys. Chem.* **1964**, *68*, 441.
- (30) Takatsuka, K.; Fueno, Y.; Yamaguchi, K. *Theor. Chim. Acta* **1978**, *48*, 175.
- (31) See also: Staroverov, V. N.; Davidson, E. R. *Chem. Phys. Lett.* **2000**, *330*, 161.
- (32) (a) Head-Gordon, M. *Chem. Phys. Lett.* **2003**, *372*, 508. (b) Head-Gordon, M. *Chem. Phys. Lett.* **2003**, *380*, 488.
- (33) Plasser, F.; Pašalić, H.; Gerzabek, M. H.; Libisch, F.; Reiter, R.; Burgdorfer, J.; Müller, T.; Shepard, R.; Lischka, H. *Angew. Chem., Int. Ed.* **2013**, *52*, 2581.
- (34) Beneberu, H. Z.; Tian, Y.-H.; Kertesz, M. *Phys. Chem. Chem. Phys.* **2012**, *14*, 10713.
- (35) Gogonea, V.; Schleyer, P. v. R.; Schreiner, P. R. *Angew. Chem., Int. Ed.* **1998**, *37*, 1945.
- (36) Mantina, M.; Chamberlin, A. C.; Valero, R.; Cramer, C. J.; Truhlar, D. G. *J. Phys. Chem. A* **2009**, *113*, 5806.
- (37) Choi, C. H.; Kertesz, M. *Chem. Commun.* **1997**, 2199.
- (38) Kaupp, G.; Boy, J. *Angew. Chem., Int. Ed. Engl.* **1997**, *36*, 48.
- (39) Isea, R. *THEOCHEM* **2001**, *540*, 131.